Journal of Geography and Geology; Vol. 14, No. 1; 2022
ISSN 1916-9779 E-ISSN 1916-9787
Published by Canadian Center of Science and Education

Classification and Mapping of Plant Communities Using Multi-Temporal and Multi-Spectral Satellite Images

Ram C. Sharma[1], Hidetake Hirayama[1], Masatsugu Yasuda[2], Miki Asai[2] & Keitarou Hara[1]

[1] Department of Informatics, Tokyo University of Information Sciences, Chiba, Japan

[2] Asia Air Survey Co., Ltd., Kawasaki city, Kanagawa, Japan

Correspondence: Ram C. Sharma, Department of Informatics, Tokyo University of Information Sciences, 4-1 Onaridai, Wakaba-ku, Chiba 265-8501, Japan. Tel: 81-43-236-4603. E-mail: sharma@rsch.tuis.ac.jp

Received: April 1, 2022 Accepted: April 29, 2022 Online Published: May 11, 2022

doi: 10.5539/jgg.v14n1p43 URL: https://doi.org/10.5539/jgg.v14n1p43

Abstract

Classification and mapping of plant communities is an essential step for conservation and management of ecosystems and biodiversity. We adopt the Genus-Physiognomy-Ecosystem (GPE) system developed in the previous study for satellite-based classification of plant communities at a broad scale. This paper assesses the potential of multi-spectral and multi-temporal images collected by Sentinel-2 satellites for the classification and mapping of GPE types. This research was conducted in seven representative study sites in different climatic regions ranging from one warm-temperate site in Aya to six cool-temperate sites in Hakkoda, Zao, Oze, Shirakami, Kitakami and Shiranuka. The GPE types were enumerated in all study sites and ground truth data were collected with reference to extant vegetation surveys, visual interpretation of high-resolution images, and onsite field observations. We acquired all Sentinel-2 Level-1C product images available for the study sites between 2017-2019 and generated monthly median composite images consisting of ten spectral and twelve spectral-indices. The Gradient Boosting Decision Trees (GBDT) classifier was employed for the supervised classification of the satellite data with the support of ground truth data. The cross-validation accuracy in terms of kappa coefficient varied from 87% in Oze site with 41 GPE types to 95% in Hakkoda site with 19 GPE types; with average performance of 91% across all sites. The GPE maps produced in this research demonstrated a clear distribution of plant communities in all seven sites, highlighting the potential of Sentinel-2 multi-spectral and multi-temporal images with GPE classification system for operational and broad-scale mapping of plant communities.

Keywords: sentinel-2, vegetation, machine learning, genus-physiognomy-ecosystem, gradient boosting decision trees, Japanese archipelago

1. Introduction

Classification and mapping of plant communities is an essential step for conservation and management of ecosystems and biodiversity. In recent years, availability of free and open access data, high performance computing, and automated data processing and analysis capabilities have brought new opportunities for classification and mapping of plant communities from remotely sensed images (Murakami and Mochizuki, 2014; Wulder, 2018). In contrast to potential natural vegetation mapping based on climatic parameters available at coarse spatial resolution (Hengl et al., 2018), actual vegetation mapping (Bredenkamp et al., 1998; Su et al., 2020) with recently available satellite images can provide much detailed information at higher spatial resolution for improving the knowledge of plant community.

In Japan, a wide variety of land cover and vegetation types, ranging from Southern Subtropical Forests to Northern Arctic Meadows, exists (Numata et al., 1972; Miyawaki, 1984; Himiyama, 1998). Nationwide vegetation surveys have been conducted since 1973 and plant communities have been enumerated. First vegetation survey of the entire country was completed in 1999 with the production of vegetation survey maps at 1:50,000 scale (MoE and AAS, 1999). Since 1999, extensive field surveys have been repeated and a 1:25,000 scale vegetation survey map is being produced nationwide (Hioki, 2007). The vegetation survey follows phyto-sociological units-based organization of plant communities (Miyawaki 1968; Ohno, 2006). The plant communities are recognized through field observations and delineated in a geographical environment via a manual procedure facilitated by visual interpretation of aerial and satellite images. The manual delineation

procedure is subject to human discernment, laborious, and costly. To cope with these issues, more intelligent technology has been expected.

The major objective of this paper is to assess the potential of multi-spectral and multi-temporal images available from the Sentinel-2 mission satellites (Drusch et al, 2012) for operational and broad-scale mapping of land cover and plant community types by adopting the Genus-Physiognomy-Ecosystem (GPE) system developed in the previous study (Sharma, 2021).

2. Method

2.1 Study Sites

This research was conducted in seven representative study sites in different climatic regions countrywide ranging from one warm-temperate site in Aya to six cool-temperate sites in Hakkoda, Zao, Oze, Shirakami, Kitakami, and Shiranuka. These study sites were selected in such a way that they represent a variety of plant communities existing in the country. The location map of seven study sites has been shown in Figure 1.

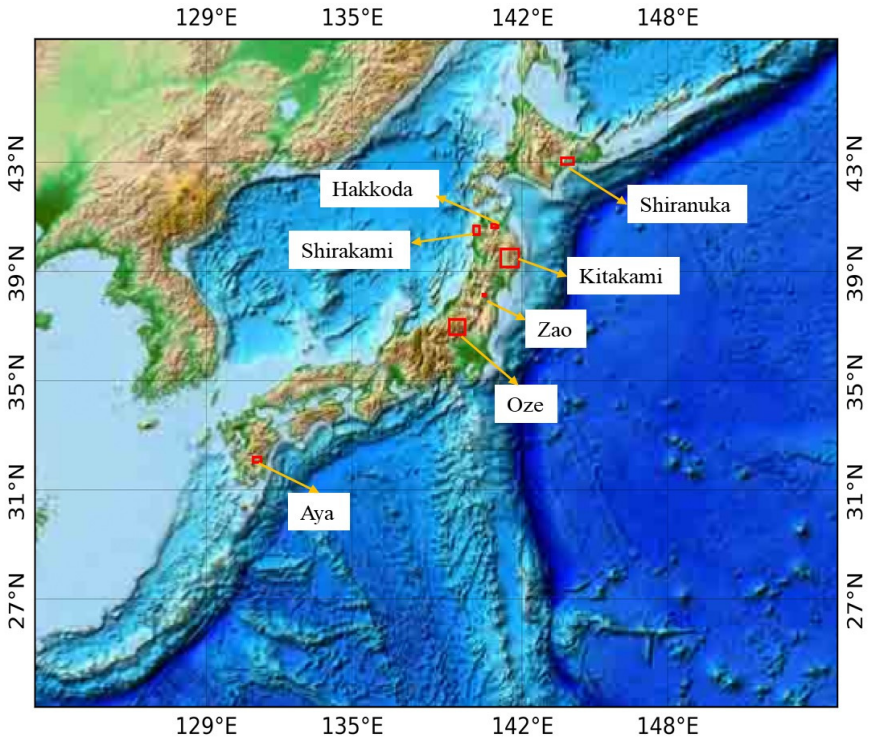

Figure 1. The location map of seven study sites: Hakkoda, Oze, Zao, Shirakami, Kitakami, Shiranuka, and Aya.

2.2 Preparation of Ground Truth Data

The land cover and plant community types present in seven study sites were enumerated by adopting the Genus-Physiognomy-Ecosystem (GPE) system developed by Sharma (2021) for satellite-based classification and mapping of plant communities at a large scale. Extant vegetation survey reports available from Nature Conservation Bureau, Ministry of the Environment and Asia Air Survey Co., Ltd were utilized as reference materials for enumerating GPE types in each study site. The land cover and plant community types were further verified by onsite field observations between 2017 and 2020 in all study sites. The final confirmed list of GPE types present in seven study sites has been described in Table 1.

Table 1. List of GPE types enumerated in seven sites. The occurrence of GPE types in each study site is denoted by the asterisk (*) symbol.

GPE types	Hakkoda	Oze	Zao	Shirakami	Kitakami	Shiranuka	Aya
Abandoned land							*
Abies ECF	*	*	*		*	*	*
Acer DBF		*	*				
Alnus DBF	*	*	*		*	*	
Alpine Herb		*	*	*	*		
Alpine Shrub			*		*		
Bamboo EBF		*			*		*
Barren	*	*	*	*	*	*	*
Betula DBF	*	*	*	*	*	*	
Carpinus DBF		*		*	*		*
Cinnamomum EBF							*
Cornus DBF							*
Cryptomeria ECF	*	*	*	*	*		*
Euptelea DBF		*					
Fagus DBF	*	*	*	*	*		*
Fraxinus DBF		*		*	*	*	
Hydrangea Shrub		*	*				
Juglans DBF		*		*	*		
Larix DCF	*	*	*	*	*	*	
Lithocarpus EBF							*
Miscanthus Herb	*	*	*	*	*		*
Openspace (Other) Herb	*	*	*	*		*	*
Deciduous (Other) Shrub	*	*	*		*	*	*
Paddy field		*		*	*		*
Pasture	*	*		*	*	*	*
Picea ECF					*	*	
Pinus ECF	*	*	*	*	*	*	*
Pinus Shrub	*	*	*	*	*		
Populus DBF		*					
Pterocarya DBF	*	*	*	*	*		*
Quercus DBF	*	*	*	*	*	*	*
Quercus EBF							*
Quercus Shrub	*	*	*	*			
Rhododendron Shrub		*			*		
Robinia DBF		*		*	*		
Salix DBF		*		*	*	*	
Salix Shrub		*	*	*	*		
Sasa Shrub	*	*	*	*	*	*	

Stewartia DBF							*
Thuja ECF		*					
Thujopsis ECF		*			*		
Tsuga ECF	*	*	*		*		
Ulmus DBF		*			*	*	
Upland field		*		*	*	*	*
Built-up (Urban)		*	*	*	*	*	*
Water		*	*	*	*	*	*
Wetland Herb	*	*	*		*	*	
Zanthoxylum DBF		*					*
Zelkova DBF		*		*	*		*
Zoysia Herb					*		
Total classes	19	41	25	26	36	19	25

DBF: Deciduous Broadleaf Forest; DCF: Deciduous Conifer Forest; ECF: Evergreen Conifer Forest; EBF: Evergreen Broadleaf Forest

The ground truth data, polygons representing homogeneous GPE types of around 1ha size, were collected with reference to extant vegetation survey maps (1:25,0000 scale) produced from extensive field surveys between 2012 to 2020, and visual interpretation of time-lapse images available in the Google Earth by local experts in plant ecology and vegetation sciences.

2.3 Processing of Satellite Data

We acquired all Level-1C product images collected by Sentinel-2 mission satellites (Sentinel-2A and 2B) for the study sites between 2017-2019. The Sentinel-2 mission satellites collect optical imagery at high spatial resolution (10-60m) in visible, near infrared, and short-wave wavelengths at a frequency of five days (Drusch et al., 2012). The images were processed for cloud masking and ten spectral bands (blue, green, red, red edge 1-3, near infrared, mid infrared, and shortwave infrared 1-2) were extracted. For each scene, twelve vegetation indices (as shown in Table 2) were also calculated. The spectral and spectral-indices images were composited by computing monthly median values. In this manner, we generated 264 features (22 spectral and spectral-indices × 12 months) altogether for machine learning, classification, and mapping.

Table 2. List of vegetation indices utilized in the research.

Spectral indices	References
Atmospherically Resistant Vegetation Index (ARVI)	Kaufman and Tanre, 1992
Enhanced Vegetation Index (EVI)	Huete et al., 2002
Green Atmospherically Resistant Index (GARI)	Gitelson et al., 1996
Green Leaf Index (GLI)	Louhaichi et al., 2001
Green Red Vegetation Index (GRVI)	Falkowski et al., 2005
Modified Red Edge Simple Ratio (MRESR)	Sims and Gamon, 2002
Modified Soil Adjusted Vegetation Index (MSAVI)	Qi et al., 1994
Normalized Difference Vegetation Index (NDVI)	Rouse et al., 1974
Optimized Soil Adjusted Vegetation Index (OSAVI)	Rondeaux et al., 1996
Red Edge Normalized Difference Vegetation Index (RENDVI)	Gitelson and Merzlyak, 2003
Soil-Adjusted Vegetation Index (SAVI)	Huete, 1988
Structure Insensitive Pigment Index (SIPI)	Penuelas et al., 1995

2.4 Machine Learning and Classification

We employed Gradient Boosting Decision Trees (GBDT) classifier implemented by XGBoost, an efficient and optimized distributed gradient boosting library (https://github.com/dmlc/xgboost) for the supervised classification of Sentinel-2 images as it can handle large data volume with Compute Unified Device Architecture (CUDA) computations. We implemented a train-test split method for fine tuning of input features and model parameters. Classification accuracy metrics (Kappa coefficient and F1-score) were utilized for quantitative evaluation. For this method, ground truth data were shuffled and randomly splitted into train (75%) and test (25%) sets. The GBDT model was trained on the training data, whereas test data was utilized for fine tuning the parameters of the model. The GBDT model established in this was utilized for prediction and mapping of land cover and plant community types separately for each site.

3. Results

3.1 Model Test Results

The model test results obtained from the machine learning (GBDT classifier) of multi-temporal Sentinel-2 images have been shown using the confusion matrix figures (Figures 2-4) for three sites (Hakkoda, Zao, and Shirakami). Due to many classes involved, class-wise accuracy tables (Tables 3-6) have been shown for four sites (Oze, Kitakami, Shiranuka and Aya).

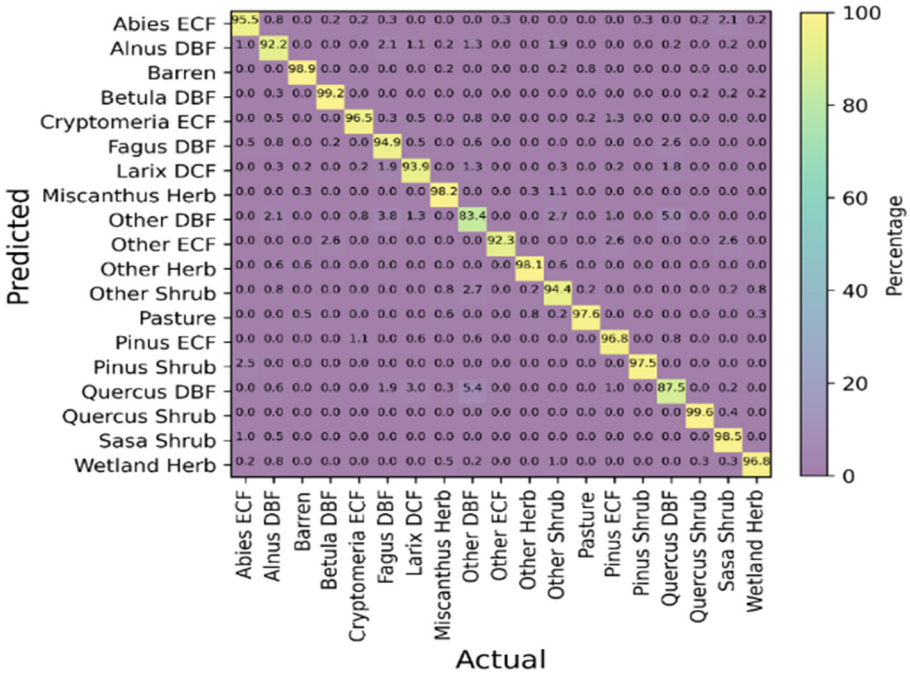

Figure 2. Confusion matrix obtained for Hakkoda site.

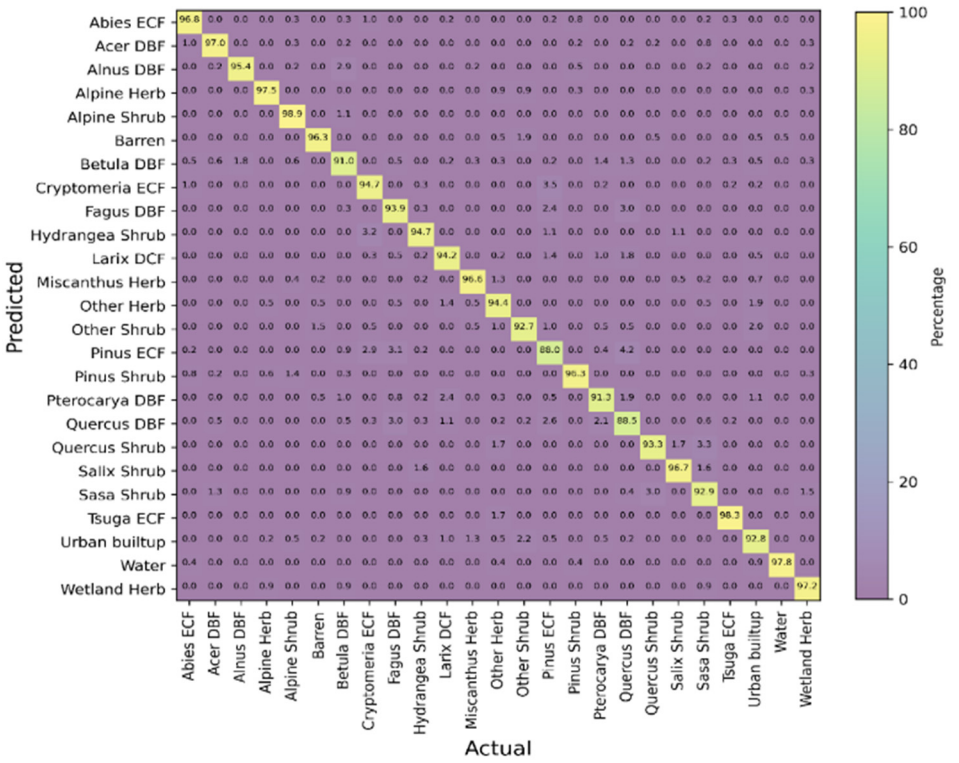

Figure 3. Confusion matrix obtained for Zao site.

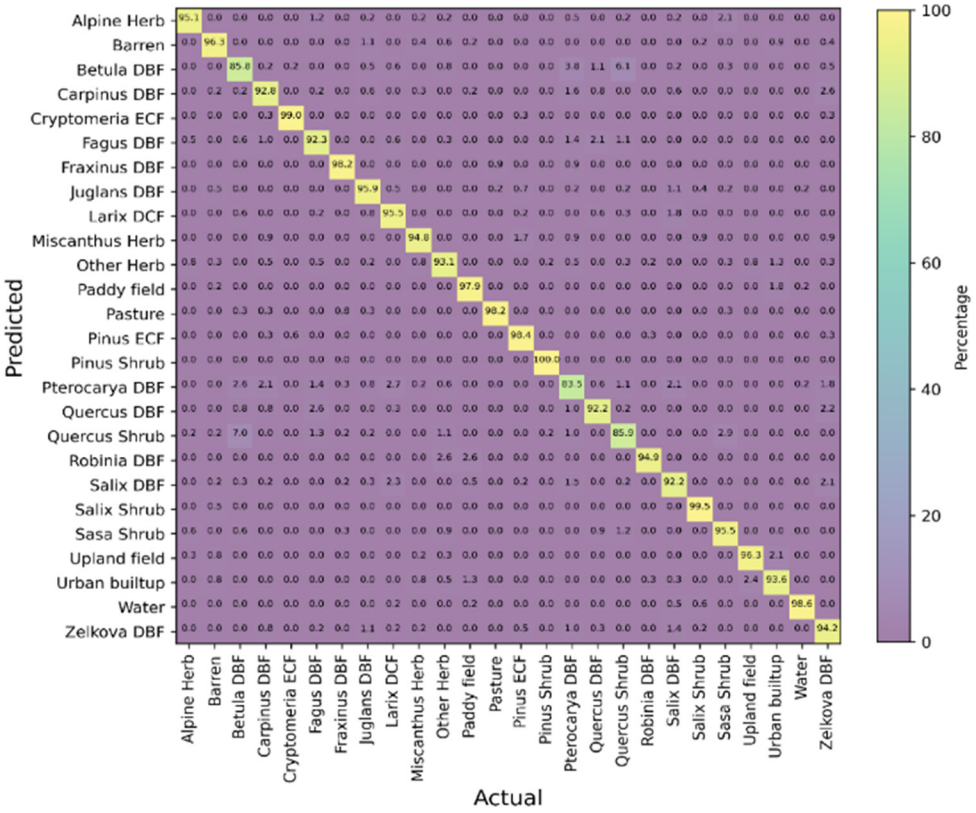

Figure 4. Confusion matrix obtained for Shirakami site.

Table 3. Class-wise accuracy obtained for Oze site.

Classes	Kappa	F1-score	Classes	Kappa	F1-score
Abies ECF	0.891	0.894	Pinus Shrub	0.782	0.783
Acer DBF	0.927	0.929	Populus DBF	0.955	0.956
Alnus DBF	0.716	0.724	Pterocarya DBF	0.760	0.766
Alpine Herb	0.927	0.929	Quercus DBF	0.785	0.791
Bamboo EBF	1.000	1.000	Quercus Shrub	0.799	0.803
Barren	0.890	0.893	Rhododendron Shrub	0.851	0.852
Betula DBF	0.766	0.772	Robinia DBF	0.967	0.968
Carpinus DBF	0.904	0.906	Salix DBF	0.879	0.883
Cryptomeria ECF	0.820	0.825	Salix Shrub	0.879	0.882
Euptelea DBF	0.882	0.885	Sasa Shrub	0.917	0.919
Fagus DBF	0.760	0.767	Thuja ECF	0.810	0.815
Fraxinus DBF	0.968	0.969	Thujopsis ECF	0.833	0.837
Hydrangea Shrub	0.718	0.726	Tsuga ECF	0.845	0.849
Juglans DBF	0.832	0.837	Ulmus DBF	0.956	0.957
Larix DCF	0.877	0.880	Upland field	0.918	0.920
Miscanthus Herb	0.870	0.873	Urban builtup	0.937	0.938
Other Herb	0.929	0.931	Water	0.992	0.992
Other Shrub	0.797	0.802	Wetland Herb	0.954	0.955
Paddy field	0.915	0.917	Zanthoxylum DBF	0.904	0.905
Pasture	0.903	0.906	Zelkova DBF	0.855	0.858
Pinus ECF	0.823	0.827			

Table 4. Class-wise accuracy obtained for Kitakami site.

Classes	Kappa	F1-score	Classes	Kappa	F1-score
Abies ECF	0.932	0.935	Pinus Shrub	0.913	0.913
Alnus DBF	0.811	0.818	Pterocarya DBF	0.885	0.889
Alpine Herb	0.964	0.966	Quercus DBF	0.820	0.827
Alpine Shrub	0.944	0.946	Rhododendron Shrub	0.976	0.976
Bamboo EBF	0.850	0.851	Robinia DBF	0.840	0.842
Barren	0.899	0.903	Salix DBF	0.885	0.889
Betula DBF	0.849	0.854	Salix Shrub	0.894	0.895
Carpinus DBF	0.946	0.948	Sasa Shrub	0.955	0.955
Cryptomeria ECF	0.929	0.932	Thujopsis ECF	0.921	0.924
Fagus DBF	0.899	0.903	Tsuga ECF	0.947	0.949
Fraxinus DBF	0.949	0.951	Ulmus DBF	0.899	0.901
Juglans DBF	0.826	0.833	Upland field	0.907	0.910
Larix DCF	0.927	0.930	Urban builtup	0.927	0.930
Miscanthus Herb	0.868	0.873	Water	0.979	0.980
Other Shrub	0.831	0.833	Wetland Herb	0.937	0.939
Paddy field	0.973	0.974	Zelkova DBF	0.878	0.882
Pasture	0.971	0.972	Zoysia Herb	0.792	0.792
Picea ECF	0.752	0.752	Zoysia Herb	0.792	0.792
Pinus ECF	0.909	0.913			

Table 5. Class-wise accuracy obtained for Shiranuka site.

Class	Kappa	F1-score	Class	Kappa	F1-score
Abies ECF	0.867	0.867	Picea ECF	0.865	0.865
Alnus DBF	0.863	0.863	Pinus ECF	0.860	0.860
Barren	0.864	0.864	Quercus DBF	0.865	0.866
Betula DBF	0.870	0.870	Salix DBF	0.850	0.851
Builtup	0.866	0.866	Sasa Shrub	0.860	0.860
Deciduous Shrub	0.870	0.870	Ulmus DBF	0.847	0.848
Fraxinus DBF	0.861	0.861	Upland Field	0.864	0.865
Larix DCF	0.865	0.866	Water	0.870	0.870
Openspace Herb	0.857	0.858	Wetland Herb	0.865	0.865
Pasture	0.866	0.867			

Table 6. Class-wise accuracy obtained for Aya site.

Class	Kappa	F1-score	Class	Kappa	F1-score
Abandoned land	0.817	0.818	Paddy field	0.964	0.964
Abies ECF	0.847	0.859	Pasture	0.966	0.967
Bamboo EBF	0.921	0.922	Pinus ECF	0.756	0.767
Barren	0.868	0.869	Pterocarya DBF	0.909	0.912
Builtup	0.960	0.961	Quercus DBF	0.947	0.948
Carpinus DBF	0.923	0.926	Quercus EBF	0.883	0.907
Chamaecyparis ECF	0.972	0.977	Shrub	0.932	0.935
Cinnamomum EBF	0.999	0.999	Stewartia DBF	0.946	0.947
Cornus DBF	0.888	0.893	Upland field	0.956	0.958
Fagus DBF	0.989	0.989	Water	0.991	0.992
Herb	0.920	0.923	Zanthoxylum DBF	0.913	0.915
Lithocarpus EBF	0.763	0.764	Zelkova DBF	0.943	0.944
Miscanthus Herb	0.818	0.821			

The classification accuracy matrices obtained for all study sites have been summarized in Table 7. The classification accuracy in terms of kappa coefficient varied from 87% in Oze site with 41 classes to 95% in Hakkoda site with 19 classes.

Table 7. Summary of classification accuracy metrics obtained for all sites.

Sites	Classes	Kappa	F1-score
Hakkoda	19	0.947	0.950
Zao	25	0.937	0.941
Oze	41	0.870	0.873
Shirakami	26	0.935	0.938
Kitakami	36	0.909	0.912
Shiranuka	19	0.874	0.875
Aya	25	0.914	0.923

3.2 GPE Maps

The Land Cover and GPE maps produced in this research have been shown in Figures 5-11. These maps demonstrate the extent and distribution of land cover and plant community types clearly for the study sites concerned.

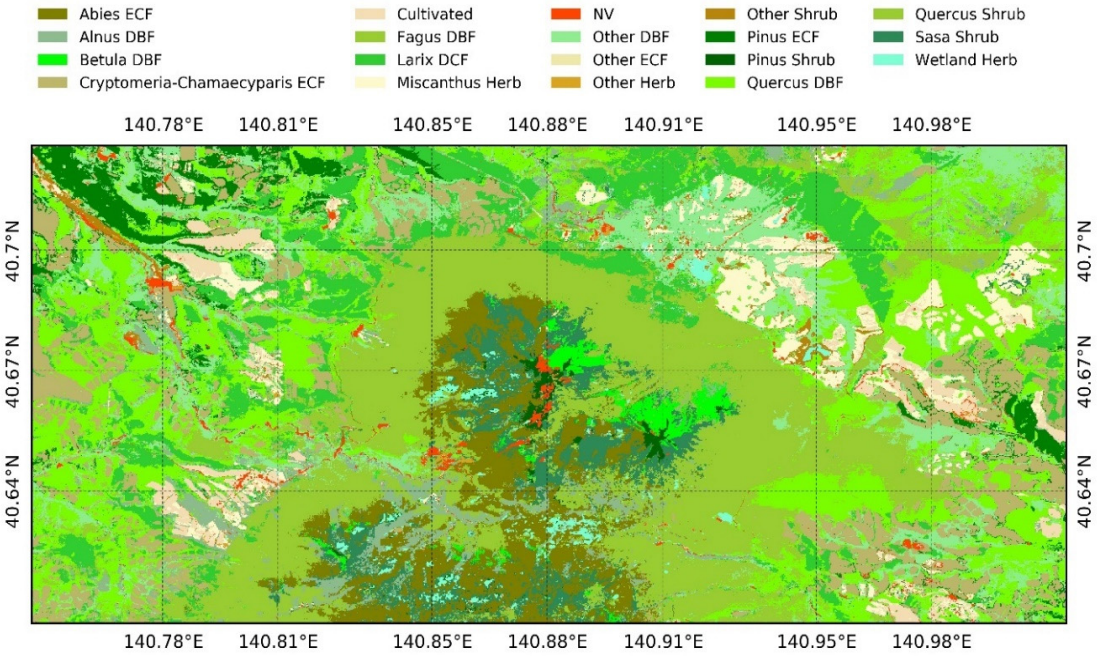

Figure 5. 19-class land cover and plant community map of Hakkoda site produced in the research.

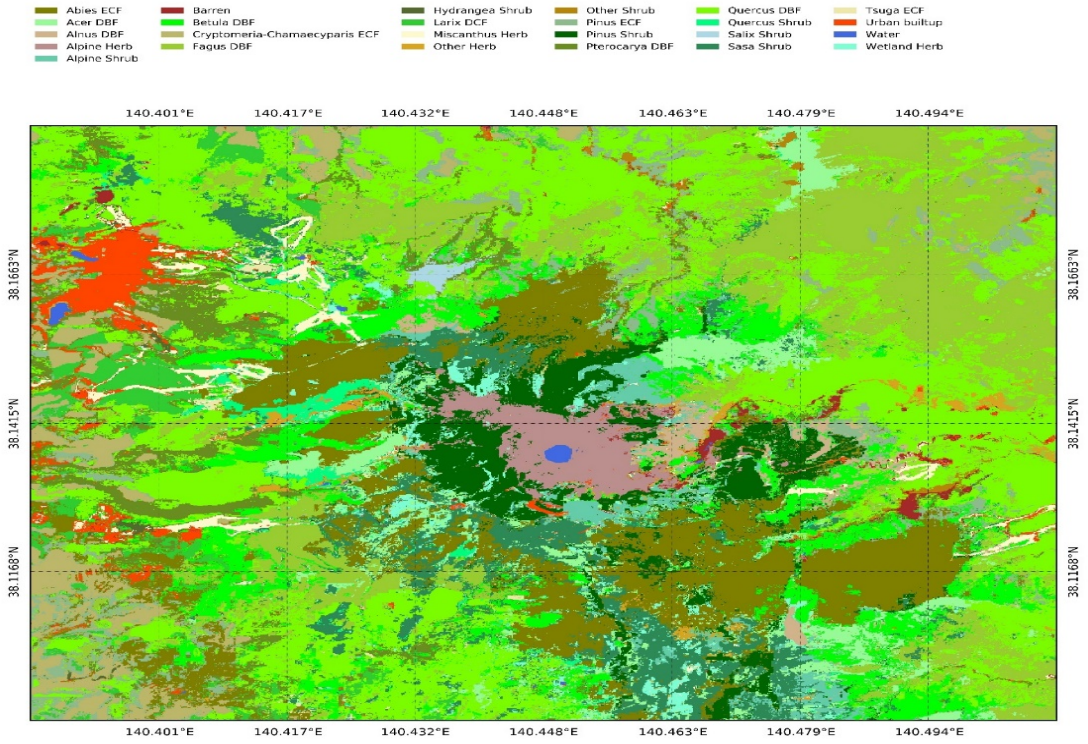

Figure 6. 25-class land cover and plant community map of Zao site produced in the research.

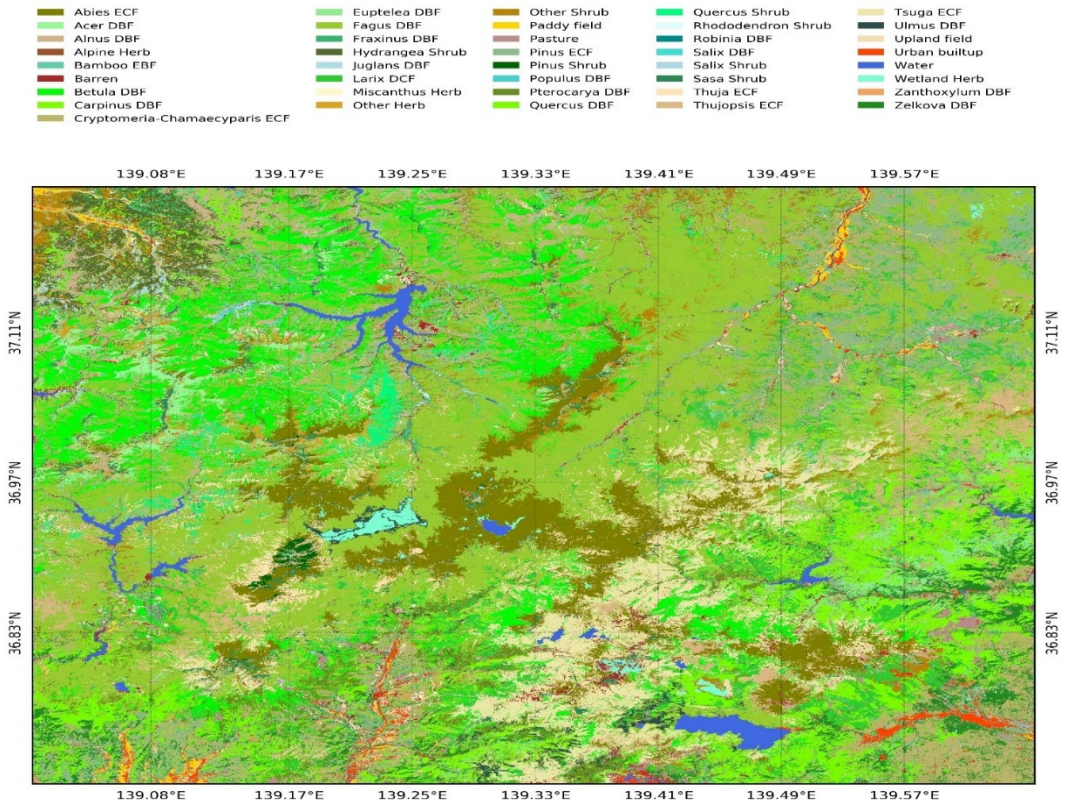

Figure 7. 41-class land cover and plant community map of Oze site produced in the research.

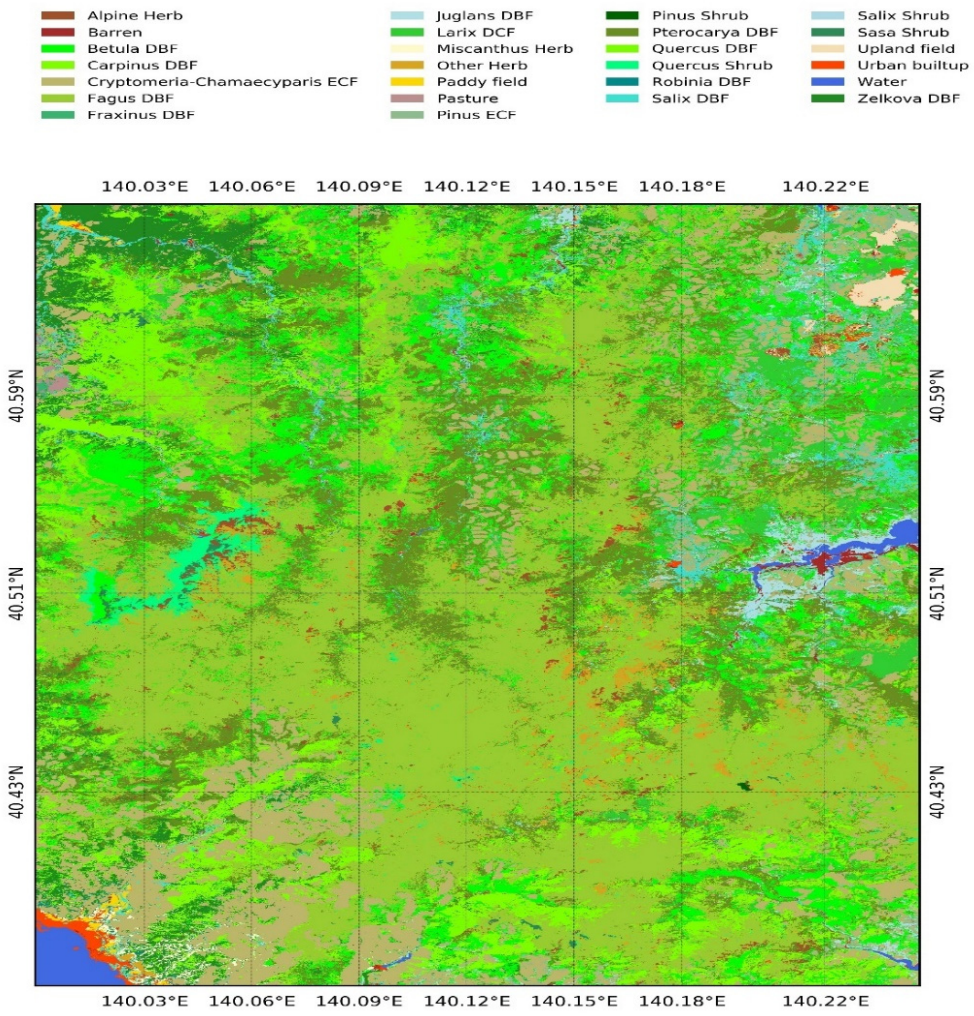

Figure 8. 26-class land cover and plant community map of Shirakami site produced in the research.

Preparation of ground truth data becomes very difficult, time-consuming, and expensive when the heterogeneity and complexity of plant community types increase. Even with the large amounts of high-quality ground truth data, classification of satellite images becomes increasingly challenging as the number of classes increases. On the other hand, the characteristic species based phyto-sociological classes (Poore, 1955; Whittaker, 1980; Miyawaki and Fujiwara, 1988) delineated by nationwide vegetation survey is out from automated digital mapping approach as remote sensing signals are mostly governed by physical interactions of dominant species rather than characteristic species. Therefore, a right and effective organization of plant communities is essential for operational and broad-scale mapping. In line with this, the Genus-Physiognomy-Ecosystem (GPE) system, developed by Sharma, 2021 for the classification of plant communities from the perspective of satellite remote sensing, was extended in this research for operational mapping of land cover and plant community types.

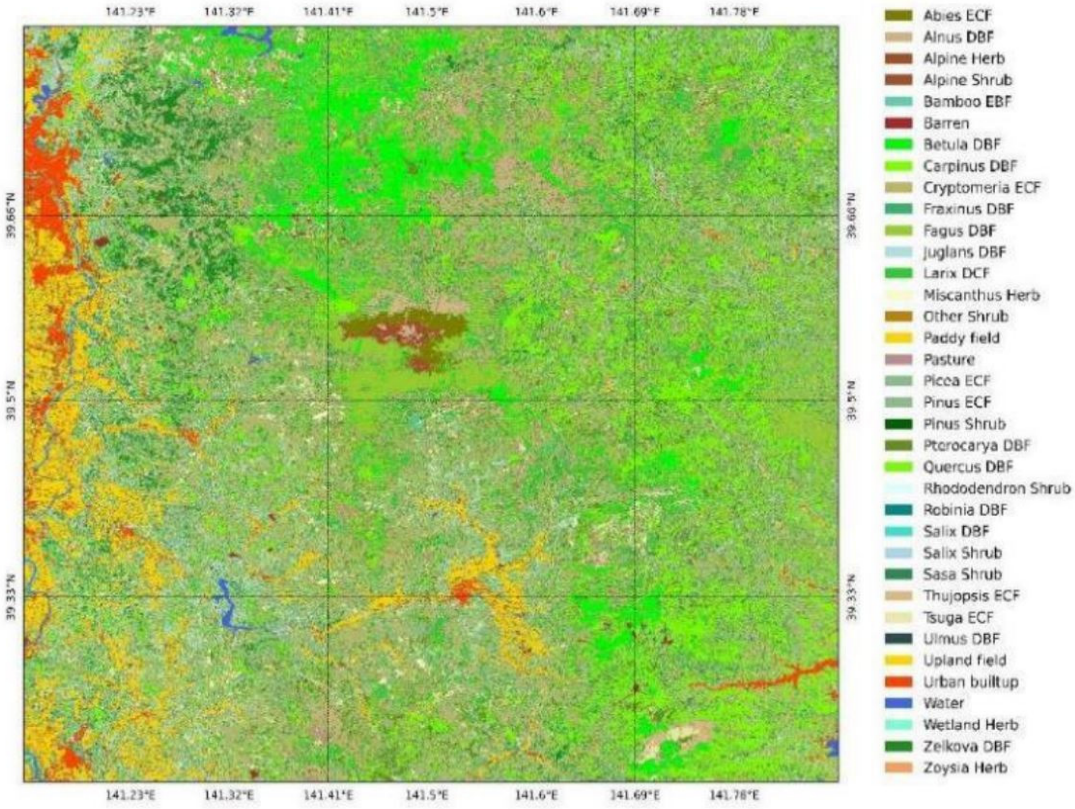

Figure 9. 36-class land cover and plant community map of Kitakami site produced in the research.

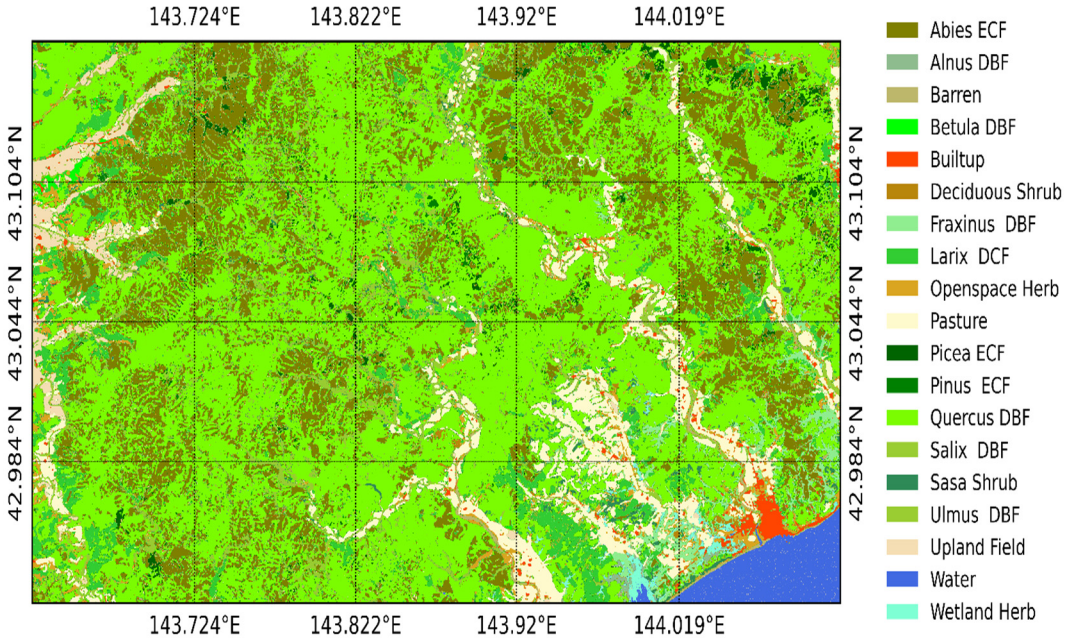

Figure 10. 19-class land cover and plant community map of Shiranuka site produced in the research.

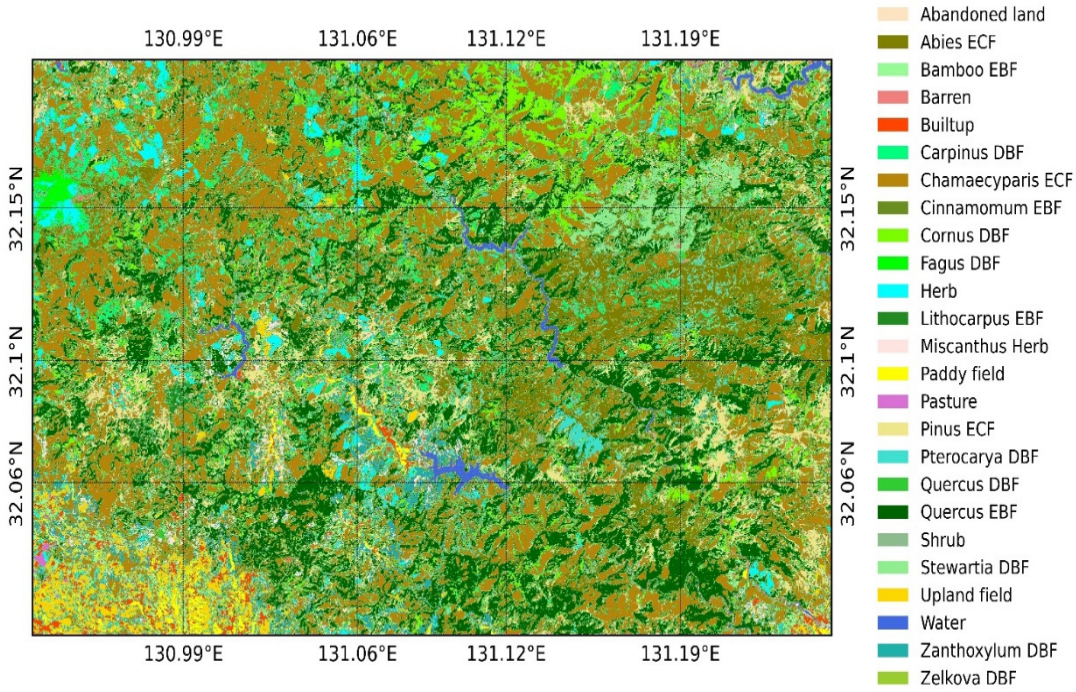

Figure 11. 25-class land cover and plant community map of Aya site produced in the research.

4. Conclusions

In this research, we presented operational mapping of land cover and plant community types in seven study sites in warm and cool temperate regions in Japan by utilizing multi-spectral and multi-temporal Sentinel-2 images. Machine learning based accuracy analysis showed potential of the Sentinel-2 images for the mapping of land cover and plant community types by adopting Genus-Physiognomy-Ecosystem (GPE) system as the kappa coefficient varied from 87% (41 classes in Oze site) to 95% (19 classes in Hakkoda site). Still, some misclassifications were detected in some classes such as Betula DBF, Alnus DBF, Fagus DBF, Quercus DBF, Picea ECF, Hydrangea Shrub, and Zoysia Herb particularly in sites associated with many classes. Further increase in the temporal resolution of the satellite data with future launch of Sentinel-2 mission satellites is highly expected for improving the classification accuracy of plant communities. Future plan is to expand this methodology for seamless mapping of plant communities by increasing the ground truth data.

Acknowledgments

The field data was supported by the commissioned research of the Ministry of the Environment, Center for Biodiversity and Asia Air Survey Co., Ltd. This research was partially supported by JSPS Grant-in-Aid for Scientific Research (JP19H04320). R. Sharma conceptualized the research, performed the research, and wrote the manuscript. H. Hirayama assisted in data processing. M. Yasuda and M. Asai assisted in the organization and collection of groundtruth data. K. Hara supervised the research. All authors have read and agreed to the published version of the manuscript.

References

Bredenkamp, G., Chytrý, M., Fischer, H. S., Neuhäuslová, Z., & van der Maarel, E. (1998). Vegetation Mapping: Theory, Methods and Case Studies: Introduction. *Applied Vegetation Science, 1*(2), 162–164. JSTOR. https://doi.org/10.1111/j.1654-109X.1998.tb00397.x

Drusch, M., Del Bello, U., Carlier, S., Colin, O., Fernandez, V., Gascon, F., Hoersch, B., Isola, C., Laberinti, P., & Martimort, P. (2012). Sentinel-2: ESA's optical high-resolution mission for GMES operational services. *Remote Sensing of Environment, 120*, 25–36. https://doi.org/10.1016/j.rse.2011.11.026

Falkowski, M. J., Gessler, P. E., Morgan, P., Hudak, A. T., & Smith, A. M. S. (2005). Characterizing and mapping forest fire fuels using ASTER imagery and gradient modeling. *Forest Ecology and Management, 217*(2–3), 129–146. https://doi.org/10.1016/j.foreco.2005.06.013

Gitelson, A. A., Gritz †, Y., & Merzlyak, M. N. (2003). Relationships between leaf chlorophyll content and spectral reflectance and algorithms for non-destructive chlorophyll assessment in higher plant leaves. *Journal of Plant Physiology, 160*(3), 271–282. https://doi.org/10.1078/0176-1617-00887

Gitelson, A. A., Kaufman, Y. J., & Merzlyak, M. N. (1996). Use of a green channel in remote sensing of global vegetation from EOS-MODIS. *Remote Sensing of Environment, 58*(3), 289–298. https://doi.org/10.1016/S0034-4257(96)00072-7

Hengl, T., Walsh, M. G., Sanderman, J., Wheeler, I., Harrison, S. P., & Prentice, I. C. (2018). Global mapping of potential natural vegetation: An assessment of machine learning algorithms for estimating land potential. *PeerJ, 6*, e5457. https://doi.org/10.7717/peerj.5457

Himiyama, Y. (1998). Land use/cover changes in Japan: From the past to the future. *Hydrological Processes, 12*(13-14), 1995–2001. https://doi.org/10.1002/(SICI)1099-1085(19981030)12:13/14<1995::AID-HYP714>3.0.CO;2-C

Hioki, Y. (2007). Issues of nation -wide actual vegetation maps from the aspect for application. *Landscape Ecology and Management, 11*(2), 107–112. https://doi.org/10.5738/jale.11.107

Huete, A. R. (1988). A soil-adjusted vegetation index (SAVI). *Remote Sensing of Environment, 25*(3), 295–309. https://doi.org/10.1016/0034-4257(88)90106-X

Huete, A., Didan, K., Miura, T., Rodriguez, E. P., Gao, X., & Ferreira, L. G. (2002). Overview of the radiometric and biophysical performance of the MODIS vegetation indices. *Remote Sensing of Environment, 83*(1–2), 195–213. https://doi.org/10.1016/S0034-4257(02)00096-2

Kaufman, Y. J., & Tanre, D. (1992). Atmospherically resistant vegetation index (ARVI) for EOS-MODIS. *IEEE Transactions on Geoscience and Remote Sensing, 30*(2), 261–270. https://doi.org/10.1109/36.134076

Louhaichi, M., Borman, M. M., & Johnson, D. E. (2001). Spatially Located Platform and Aerial Photography for Documentation of Grazing Impacts on Wheat. *Geocarto International, 16*(1), 65–70. https://doi.org/10.1080/10106040108542184

Miyawaki, A. (1968). Typen von Vegetationskarten und ihre Anwendung fur die Beurteilung des Standortes. *Map, Journal of the Japan Cartographers Association, 6*(2), 1–9.

Miyawaki, A. (1984). A vegetation-ecological view of the Japanese archipelago. *Bulletin of the Institute of Environmental Science and Technology, 11*, 85–101.

Miyawaki, A., & Fujiwara, K. (1988). Vegetation Mapping in Japan. In A. W. Küchler & I. S. Zonneveld (Eds.), *Vegetation mapping* (pp. 427–441). Springer Netherlands. https://doi.org/10.1007/978-94-009-3083-4_35

MoE. (1999). *Nature Conservation Bureau, Ministry of the Environment of Japan and Asia Air Survey Co., Ltd. The 5th National Survey on the Natural Environment (Vegetation survey) report*. Nature Conservation Bureau, Ministry of the Environment of Japan and Asia Air Survey Co., Ltd. 1999. http://www.biodic.go.jp/reports2/5th/vgtmesh/vgtmesh.html

Murakami T., & Mochizuki S. (2014). *Vegetation mapping using remotely sensed imagery*. Ecological Society of Japan. https://doi.org/10.18960/seitai.64.3_233

Numata, M., Miyawaki, A., & Itow, D. (1972). Natural and semi-natural vegetation in Japan. *Blumea, 20*(2), 435–496.

Ohno, K. (2006). Applications of a phytosociological vegetation map and its role for development with landscape ecology. *Landscape Ecology and Management, 11*(1), 39–52. https://doi.org/10.5738/jale.11.39

Penuelas, J., Frederic, B., & Filella, I. (1995). Semi-Empirical Indices to Assess Carotenoids/Chlorophyll-a Ratio from Leaf Spectral Reflectance. *Photosynthetica, 31*, 221–230.

Poore, M. E. D. (1955). The Use of Phytosociological Methods in Ecological Investigations: I. The Braun-Blanquet System. *The Journal of Ecology, 43*(1), 226. https://doi.org/10.2307/2257132

Qi, J., Chehbouni, A., Huete, A. R., Kerr, Y. H., & Sorooshian, S. (1994). A modified soil adjusted vegetation index. *Remote Sensing of Environment, 48*(2), 119–126. https://doi.org/10.1016/0034-4257(94)90134-1

Rondeaux, G., Steven, M., & Baret, F. (1996). Optimization of soil-adjusted vegetation indices. *Remote Sensing of Environment, 55*(2), 95–107. https://doi.org/10.1016/0034-4257(95)00186-7

Rouse, J. W., Haas, R. H., Schell, J. A., & Deering, D. W. (1974). Monitoring vegetation systems in the Great Plains with ERTS. *NASA Special Publication, 351*, 309.

Sharma, R. C. (2021). Genus-Physiognomy-Ecosystem (GPE) System for Satellite-Based Classification of Plant Communities. *Ecologies, 2*(2), 203–213. https://doi.org/10.3390/ecologies2020012

Sims, D. A., & Gamon, J. A. (2002). Relationships between leaf pigment content and spectral reflectance across a wide range of species, leaf structures and developmental stages. *Remote Sensing of Environment, 81*(2–3), 337–354. https://doi.org/10.1016/S0034-4257(02)00010-X

Su, Y., Guo, Q., Hu, T., Guan, H., Jin, S., An, S., Chen, X., Guo, K., Hao, Z., Hu, Y., Huang, Y., Jiang, M., Li, J., Li, Z., Li, X., Li, X., Liang, C., Liu, R., Liu, Q., … Ma, K. (2020). An updated Vegetation Map of China (1:1000000). *Science Bulletin, 65*(13), 1125–1136. https://doi.org/10.1016/j.scib.2020.04.004

Whittaker, R. H. (1980). *Classification of Plant Communities*. Springer Netherlands. https://doi.org/10.1007/978-94-009-9183-5

Wulder, M. A., Coops, N. C., Roy, D. P., White, J. C., & Hermosilla, T. (2018). Land cover 2.0. *International Journal of Remote Sensing, 39*(12), 4254–4284. https://doi.org/10.1080/01431161.2018.1452075